

Inversion of Growth Speed Anisotropy in Two Dimensions

Thomas Michely, Michael Hohage, Michael Bott, and George Comsa
Institut für Grenzflächenforschung und Vakuumphysik, Kernforschungsanlage Jülich,
Postfach 1913, 5170 Jülich, Germany
 (Received 22 February 1993)

An inversion of the triangular shapes of the two-dimensional islands observed in a narrow temperature range by scanning tunneling microscopy during growth of Pt on Pt(111) is reported. This phenomenon is due to the inversion of the growth speed ratio of the two types of close packed $\langle 110 \rangle$ step edges. It is tentatively traced back to an inversion in the hierarchy of the atom diffusion speeds along the two types of step edges in this temperature range.

PACS numbers: 68.35.Bs, 61.16.Ch, 68.35.Fx, 68.55.Jk

During molecular beam homoepitaxy the supersaturation in the gas phase above the crystal surface is extremely high. Correspondingly, the supersaturation of the two-dimensional (2D) adatom lattice gas is also high, except at too high surface temperature. As a consequence stable nuclei are formed on the terraces which then grow to islands [1]. In view of the 2D supersaturation, the shapes of the 2D islands are determined by the kinetics of the 2D growth process, which in turn is determined by the onset and relative importance of thermally activated diffusion processes.

We report here on a study of the island shapes of Pt islands grown on Pt(111) at various surface temperatures T_s and submonolayer coverages. We will show that for $T_s < 700$ K the island shapes are growth shapes, i.e., determined by the kinetics during growth, while for $T_s > 700$ K the shape corresponds to a local 2D equilibrium. In particular we report a new phenomenon, the temperature-dependent inversion of the growth speed anisotropy.

A glance onto the scanning tunneling microscope (STM) images in Fig. 1 makes the drastic influence of the substrate temperature T_s on the island shape obvious. Figures 1(b) and 1(d), obtained upon deposition at 400

and 640 K, respectively, both show essentially triangular islands. However, the triangles in 1(b) seem to be the mirror image of the triangles in 1(d). This switch in the triangle orientation appears to be due to a temperature-dependent inversion of the growth speed anisotropy. We speculate that this effect can be understood by the temperature dependence of the Pt atom diffusion along steps.

The experiments were performed in a UHV chamber equipped with standard facilities (low-energy electron diffraction, Auger electron spectroscopy, etc.) and a specially designed variable temperature STM. The STM and the apparatus are described in detail elsewhere [2]. The vapor phase deposition of Pt was performed at various surface temperatures T_s by sublimation of a Pt foil, heated by electron bombardment. The deposited amount Θ specified in fractions of a monolayer (ML) is inferred from the evaluation of the island covered area in the STM images after deposition. When the desired amount has been deposited, the sample is quenched. The frozen-in morphology is then investigated by STM.

The discussion of the island shapes of Figs. 1(a) and 1(e) will set the framework for the further analysis. Figure 1(a), obtained after deposition at 200 K, exhibits similar growth shapes as those observed for Au on

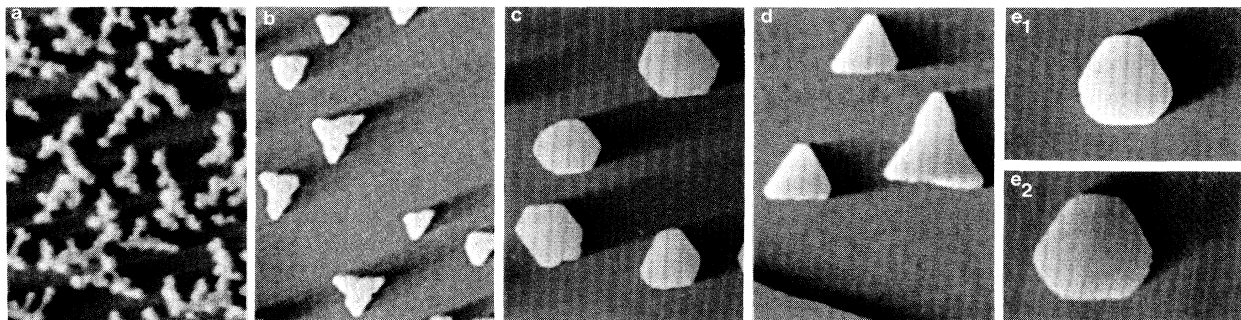


FIG. 1. Island shapes on Pt(111) resulting at various surface temperatures T_s after deposition of an amount Θ with a typical rate of 1×10^{-2} ML/s on images with a size S . (a) $T_s = 200$ K, $\Theta = 0.2$ ML, $S = 280 \text{ \AA} \times 400 \text{ \AA}$; (b) $T_s = 400$ K, $\Theta = 0.08$ ML, $S = 1300 \text{ \AA} \times 1900 \text{ \AA}$; (c) $T_s = 455$ K, $\Theta = 0.14$ ML, $S = 770 \text{ \AA} \times 1100 \text{ \AA}$; (d) $T_s = 640$ K, $\Theta = 0.15$ ML, $S = 2300 \text{ \AA} \times 3300 \text{ \AA}$; (e₁) $T_s = 710$ K, $\Theta = 0.08$ ML, $S = 1540 \text{ \AA} \times 1100 \text{ \AA}$; (e₂) after deposition at $T_s = 425$ K ($\Theta = 0.08$ ML) the sample was *additionally annealed* to 710 K for 1 min and then imaged ($S = 630 \text{ \AA} \times 900 \text{ \AA}$).

Ru(0001) by Hwang *et al.* [3]: Each island exhibits a branched structure with a branch thickness that is small compared to the diameter of the smallest circle containing the island. The branches are *not* correlated to the orientation of the substrate. The branch thickness down to atomic dimensions and the atomic roughness of the island ledges indicate the absence of step edge diffusion [4]. Accordingly the island shape on Pt(111) at 200 K appears to be a physical realization of the “hit-and-stick” mechanism used in the computer simulation of 2D fractals [5]. Indeed, the activation energies for adatom migration on the (111) terrace of Pt and for diffusion of atoms along step edges on this surface are of the order of 0.1 eV and > 0.5 eV, respectively [6]. Assuming an accommodation probability of one at 200 K [in accordance with recent field ion microscope (FIM) results [7]], the mobile adatoms stick at the point of the first impact to the island ledge, the step edge diffusion being ruled out by its high activation energy. It is this gap between the activation energies for migration and step edge diffusion that appears to allow for 2D fractal growth. From the diffusion data for other fcc metals [8] it can be expected that the 2D fractal growth on the (111) terrace is a common phenomenon in homoepitaxy.

The islands resulting upon growth at 700 K exhibit a regular hexagonal shape of threefold symmetry [Fig. 1(e₁)] bounded by two types of steps (*A* and *B* steps) with atomically different structure (see ball model in Fig. 2 for the terminology). The unique island shape above 700 K is identical for adatom and vacancy islands [9] and is independent of its history; i.e., the same shape results whether the islands have been grown at 700 K [Fig. 1(e₁)] or grown at another temperature and then annealed to 700 K [Fig. 1(e₂)]. An analysis similar to that performed for the vacancy islands on Pt(111) shows that the adatom islands above 700 K are close to their equilibrium shape with a step free energy ratio of $\delta^A/\delta^B = 0.87 \pm 0.02$ [9,10]. A steep rise in the 2D vapor pressure of the island ledges has been identified as the mechanism leading to island shape equilibration [11]. At deposition temperatures $T_s < 700$ K the islands are not equilibrium shaped. They are growth shapes determined by the growth kinetics.

We address now the main topic of this Letter, the in-

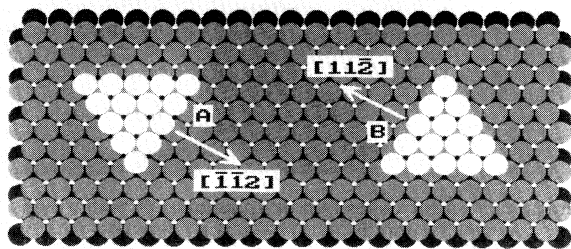


FIG. 2. Ball model of two small adatom islands bounded either by *A* steps (a Δ_l island) or *B* steps (a Δ_h island).

version of the growth speed anisotropy in the deposition temperature range $350 < T_s < 650$ K, as evidenced in the 180° inversion of the island shape. Despite some roughness, the island shapes grown at 400 K in Fig. 1(b) and at 640 K in Fig. 1(d) are both essentially triangular. However, the low-temperature triangles (Δ_l islands) are mainly bounded by *A* steps whereas the high-temperature triangles (Δ_h islands) are bounded by *B* steps. In the temperature range between 450 and 470 K a hexagonal transition shape is observed [Fig. 1(c)]. It is obvious in analogy to the three-dimensional case [12] that only those boundaries (step edges) of the 2D islands which advance the slowest will survive during the growth process. Let us define the speed of advancement in the direction normal to the step edges *A* and *B* as the growth speeds $v_{[\bar{1}\bar{1}2]}$ and $v_{[11\bar{2}]}$, respectively (see Fig. 2). The hexagonal transition shape indicates that in the range $450 < T_s < 470$ K the step edges *A* and *B* advance with nearly the same speed, i.e., the ratio of speeds $r_{\text{hex}} = v_{[\bar{1}\bar{1}2]}/v_{[11\bar{2}]} \approx 1$. Simple geometrical considerations show that triangular shapes like those in Figs. 1(b) and 1(d) are obtained for $r(\Delta_l) \leq \frac{1}{2}$ and $r(\Delta_h) \geq 2$, respectively. This means that within a narrow temperature range of 440 to 480 K the advancement speed anisotropy of the step edges is inverted, the ratio *r* varying by at least a factor of 4. In the following, we will analyze three possible causes of this substantial change.

Mo *et al.* [13] have demonstrated that the anisotropic shape of Si islands on Si(100) can be explained and simulated by the assumption of anisotropic accommodation of the arriving adatoms at the island ledge. In the discussion of the fractal island shapes obtained at 200 K we could assume [7] that the accommodation probability is unity. At the higher temperatures now under consideration ($T_s > 350$ K) this probability might deviate from unity and may depend on the island step orientation. Such a behavior could explain the growth of triangular island shapes. However, we can hardly imagine any physical reason for a temperature-dependent inversion of this possible anisotropy of accommodation which would be large enough to explain the switch of *r* from $\leq \frac{1}{2}$ to ≥ 2 .

At higher temperatures step atoms may reevaporate onto the terrace. An anisotropy of the evaporation rate might also cause an anisotropic growth speed during deposition. The step type with the higher evaporation rate would grow slower and hence be present in the final shape. If this mechanism is operative, keeping the surface at the deposition temperature after the end of deposition, it should, if at all, only change the island shape towards a greater anisotropy. Experimentally just the opposite is observed: The Δ_l as well as the Δ_h islands tend to change their shape towards a more hexagonal shape. Note that this type of experiment also demonstrates that the Δ_l or Δ_h islands do not have an equilibrium shape. Thus the inversion of the shape is not due to a tem-

perature-dependent step free energy anisotropy.

We come finally to what we consider to be the main cause for the observed phenomena: the anisotropy of step edge diffusion, i.e., the different speeds of migration of atoms along differently oriented steps. We have direct evidence that step edge diffusion is operative in the temperature range considered: Annealing the fractal islands obtained at 200 to 400 K causes substantial changes of their shape. The diffusion along the dense packed steps on the (111) face of an fcc crystal, i.e., the $\langle 110 \rangle$ oriented A and B steps, is known to be faster than along steps with any other orientation. As a simplified model, we consider now the growth of a more or less circular seed island and assume for the moment identical diffusion speeds along A and B steps. An adatom arriving at any rough part of the island ledge will immediately be trapped by a nearby kink. In contrast an adatom arriving at an A or B step will migrate along it and finally be trapped at a kink site at the end of the dense packed step. Thereby the dense packed step edge becomes larger but does not advance normal to itself. This very rough picture allows one to understand why the dense packed steps do develop during growth and how a circular seed becomes a hexagonal island. The difference in the advancement speed of the two types of $\langle 110 \rangle$ step edges A and B , which explains the triangular shapes observed, can be traced back to a difference between the migration speeds of the atoms along the step edges A and B . Indeed, the lower the adatom migration speeds along a step edge, the higher the density of step adatoms; and further, the higher the density, the higher the probability of nucleation of a new step edge line and thus the speed of advancement of that step edge. In summary, the lower the speed of migration along a given step edge, the higher the speed of advancement of this step edge. From Fig. 1(b) where the edges of the Δ_l islands are of A type we conclude that at lower temperature the diffusion coefficient along the A step edges D^A should be larger than that along the B step edges D^B , while from Fig. 1(d) just the opposite ($D^B > D^A$) should be true. Basset and Webber [6] have

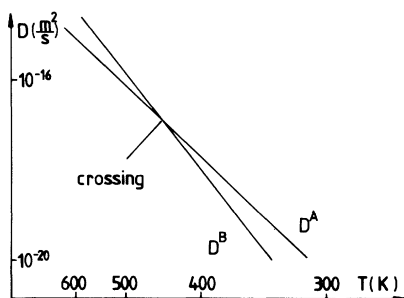


FIG. 3. Temperature dependence of the diffusion coefficient D^A for atom diffusion along A -type channels on Pt(331) and of D^B for atom diffusion along B -type channels on Pt(113) based on the data of Ref. [6].

measured the diffusion of Pt atoms along the channels of the Pt(113) and (331) surfaces, which have a structure identical to that of the step edges A and B , respectively. The diffusion coefficients for the adatom migration along the two types of step edges as obtained from the data given in Table 1 of Ref. [6] are plotted in Fig. 3 as a function of temperature. They fully confirm the anisotropy of the diffusion and its inversion as deduced from the arguments above. The coincidence between the temperature at which $D^A = D^B$ with the narrow temperature range in which the hexagonal islands (equal advancement speeds) are observed [Fig. 1(c)] is very nice, but should not be overvalued: The activation energies for diffusion and the corresponding preexponentials have been determined in Ref. [6] only at low temperatures, so that Fig. 3 is an extrapolation involving certainly a large error margin. Nevertheless, a similar behavior of the diffusion coefficients D^A and D^B , which allows one to expect $D^A > D^B$ at low temperatures and $D^B > D^A$ at higher temperatures, has been observed for all fcc (111) surfaces investigated so far [8]. According to our speculation, the temperature where the hexagonal transition shape is observed is determined by $D^A = D^B$. Thus this temperature should be largely independent of the deposition rate. This has been checked by varying the deposition rate over 2 orders of magnitude. We have also performed Monte Carlo calculations to simulate the island growth up to temperatures of 650 K. With a single set of parameters,

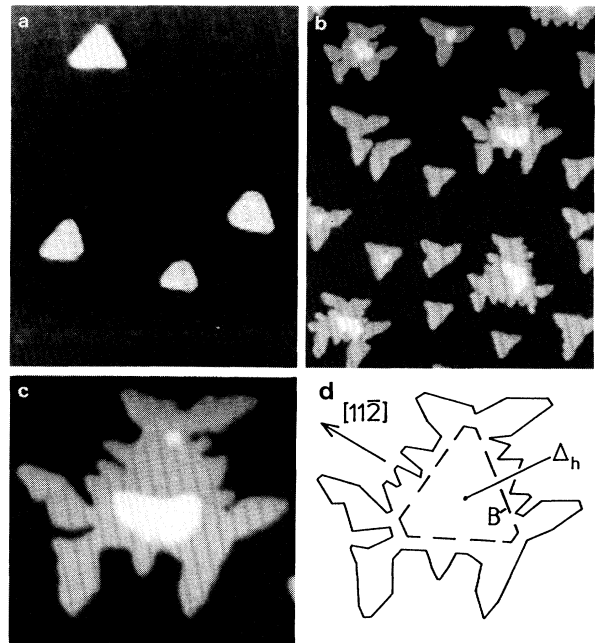


FIG. 4. (a) $T_s = 600$ K, $\Theta = 0.04$ ML, $R = 3.3 \times 10^{-3}$ ML/s, $S = 2100 \text{ \AA} \times 3150 \text{ \AA}$. (b) Same sample as in (a) but after additional deposition of $\Theta = 0.16$ ML, at $T_s = 400$ K. (c) Enlarged section of (b) with $S = 750 \text{ \AA} \times 750 \text{ \AA}$. (d) Sketch of the hybrid island (see text) of (c), where the initial Δ_h island is dashed.

consistent with the diffusion data from Ref. [6], the essential features of the island shape evolution were reproduced satisfactorily. These simulations and additional experimental details will be presented in a forthcoming publication [14].

Before we leave the analysis of Fig. 1, let us note one more aspect present in the STM images. It is apparent in Figs. 1(b) and 1(d) that the largest islands in each image are no longer triangles but exhibit concave sides. The triangle corners seem to accelerate their rate of advancement during growth. In fact, once the triangular shape is developed a new effect becomes significant: The adatom concentration field around an island will show the steepest gradient in the proximity to the corners [15]. Thus, compared to the sides, the corners of the triangles receive an increased supply of adatoms. With the increasing length of the island edges the mass transport along them can hardly cope with this increased supply so that tip formation and self-accelerated growth of the triangle corners set in [15].

Instead of a summary, we give an experimental illustration of the foregoing discussion. In Fig. 4(a) we deposited 4% of a ML at 600 K and a Δ_h island resulted (B steps). After that the temperature was set at 400 K and another 16% of a ML was deposited [Fig. 4(b)]: Many new Δ_l islands are visible together with a number of hybrid islands having about the same low density as the initial 600 K Δ_h islands. Figure 4(c) shows one of the hybrid islands in higher magnification. As sketched in Fig. 4(d) the atoms attached at 400 K to the 600 K Δ_h island give rise to the hybrid appearance. At 400 K the B sides of the Δ_h island are sides of slow diffusion. At the corners of the initial Δ_h island the overall mass supply at 400 K is largest and thus the largest amount of material is attached there: Δ_l islands grow out from the three corners of the Δ_h island. Additionally the atoms incorporated into the sides of the Δ_h island (B steps) form small Δ_l -like islands pinned to the step edge with a typical separation determined by the low diffusion speed along this step type. The design of this hybrid island exemplifies three aspects of our discussion: The inversion of the growth speed anisotropy is verified directly, the im-

portant role of step edge diffusion is apparent, and finally the enhanced material supply to corners can be deduced straightforwardly.

We have benefited from the experimental help of Stefanie Esch and Christian Teichert as well as of stimulating discussions with Bene Poelsema and Mario Jakas.

-
- [1] M. Bott, Th. Michely, and G. Comsa, *Surf. Sci.* **272**, 161 (1992).
 - [2] K. H. Besocke, *Surf. Sci.* **181**, 145 (1987); Th. Michely, Forschungszentrum Jülich Jül-Bericht 2569, 1991.
 - [3] R. Q. Hwang, J. Schröder, C. Günther, and R. J. Behm, *Phys. Rev. Lett.* **67**, 3279 (1991).
 - [4] In the case of Au deposited on Ru(0001) at room temperature the branch thickness of 50 to 100 Å and the radii of curvature of the same order indicate that a non-negligible step edge diffusion during growth was still present [3].
 - [5] T. A. Witten and L. M. Sander, *Phys. Rev. B* **27**, 5686 (1983).
 - [6] D. W. Basset and P. R. Webber, *Surf. Sci.* **70**, 520 (1978).
 - [7] S. C. Wang and G. Ehrlich, *Phys. Rev. Lett.* **70**, 41 (1993).
 - [8] G. Ayrault and G. Ehrlich, *J. Chem. Phys.* **60**, 281 (1974); R. T. Tung and W. R. Graham, *Surf. Sci.* **97**, 73 (1980); S. C. Wang and G. Ehrlich, *Surf. Sci.* **239**, 301 (1990).
 - [9] Th. Michely and G. Comsa, *Surf. Sci.* **256**, 217 (1991).
 - [10] M. Bott, S. Esch, M. Hohage, Th. Michely, and G. Comsa (to be published).
 - [11] Th. Michely, T. Land, U. Littmark, and G. Comsa, *Surf. Sci.* **272**, 204 (1992).
 - [12] K. Spangenberg, in *Handwörterbuch der Naturwissenschaften, Bd. 10* (Gustav Fischer Verlag, Jena, 1934), 2nd ed., p. 362, or W. Kleber, *Einführung in die Kristallographie* (Verlag Technik, Berlin, 1990), p. 207.
 - [13] Y. W. Mo, B. S. Swartzentruber, R. Kariotis, M. B. Webb, and M. G. Lagally, *Phys. Rev. Lett.* **63**, 2393 (1989).
 - [14] M. Hohage, M. Jakas, M. Bott, Th. Michely, and G. Comsa (to be published).
 - [15] W. W. Mullins and R. F. Sekerka, *J. Appl. Phys.* **34**, 323 (1963).

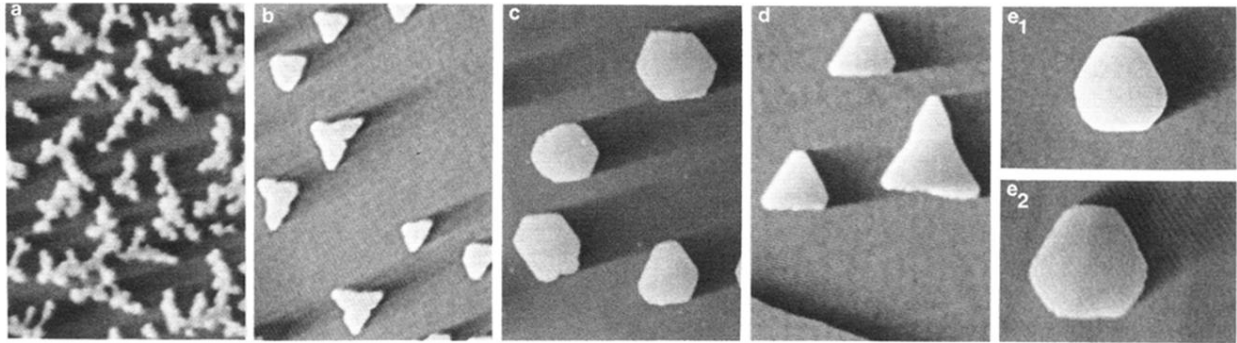


FIG. 1. Island shapes on Pt(111) resulting at various surface temperatures T_s after deposition of an amount Θ with a typical rate of 1×10^{-2} ML/s on images with a size S . (a) $T_s = 200$ K, $\Theta = 0.2$ ML, $S = 280 \text{ \AA} \times 400 \text{ \AA}$; (b) $T_s = 400$ K, $\Theta = 0.08$ ML, $S = 1300 \text{ \AA} \times 1900 \text{ \AA}$; (c) $T_s = 455$ K, $\Theta = 0.14$ ML, $S = 770 \text{ \AA} \times 1100 \text{ \AA}$; (d) $T_s = 640$ K, $\Theta = 0.15$ ML, $S = 2300 \text{ \AA} \times 3300 \text{ \AA}$; (e₁) $T_s = 710$ K, $\Theta = 0.08$ ML, $S = 1540 \text{ \AA} \times 1100 \text{ \AA}$; (e₂) after deposition at $T_s = 425$ K ($\Theta = 0.08$ ML) the sample was *additionally annealed* to 710 K for 1 min and then imaged ($S = 630 \text{ \AA} \times 900 \text{ \AA}$).

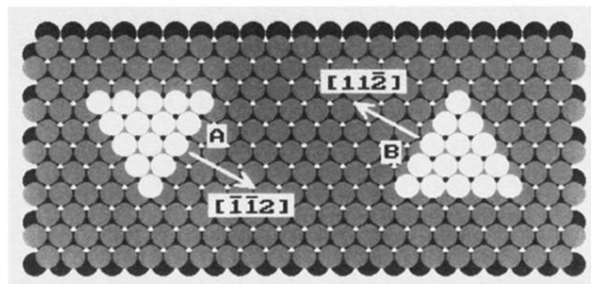


FIG. 2. Ball model of two small adatom islands bounded either by A steps (a Δ_l island) or B steps (a Δ_h island).

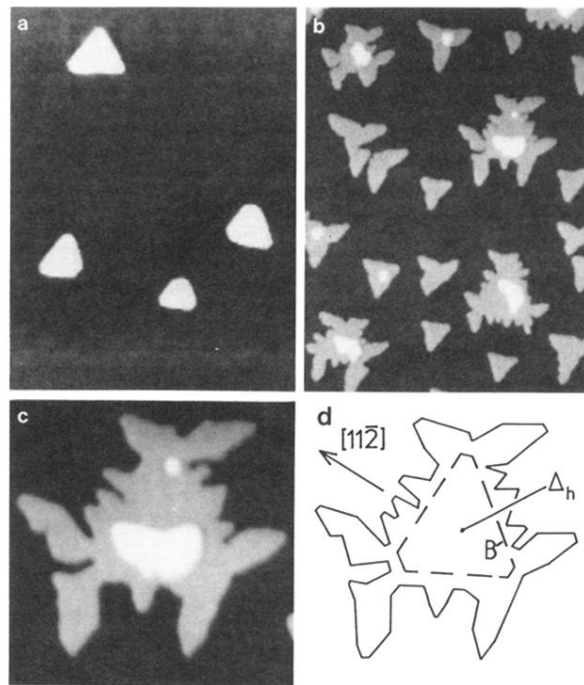


FIG. 4. (a) $T_s = 600$ K, $\Theta = 0.04$ ML, $R = 3.3 \times 10^{-3}$ ML/s, $S = 2100 \text{ \AA} \times 3150 \text{ \AA}$. (b) Same sample as in (a) but after additional deposition of $\Theta = 0.16$ ML, at $T_s = 400$ K. (c) Enlarged section of (b) with $S = 750 \text{ \AA} \times 750 \text{ \AA}$. (d) Sketch of the hybrid island (see text) of (c), where the initial Δ_h island is dashed.